

1/2

X-692-72-488

PREPRINT

NASA TM X-66187

MAGNETIC FIELD DISSIPATION IN D-SHEETS

L. F. BURLAGA
J. D. SCUDDER

(NASA-TM-X-66187) MAGNETIC FIELD
DISSIPATION IN D-SHEETS (NASA) 25 p HC
\$3.25 CSCL 03B

N73-18813

Unclas
63942

FEBRUARY 1973



— GODDARD SPACE FLIGHT CENTER —
GREENBELT, MARYLAND

X-692-72-488

MAGNETIC FIELD DISSIPATION IN D-SHEETS

L. F. Burlaga
J. D. Scudder

Laboratory for Extraterrestrial Physics
NASA-Goddard Space Flight Center
Greenbelt, Maryland 20771

February 1973

I

Abstract

This paper examines the effects of magnetic field annihilation at a tangential or rotational discontinuity in a resistive plasma. The magnetic field intensity profile depends on : 1) the field intensities, B_{∞}^{\pm} , far from the current sheet (directional discontinuity); 2) the angle ω between B_{∞}^{+} and B_{∞}^{-} ($B_{\infty}^{-}/B_{\infty}^{+} \equiv < 1$); and 3) the electrical resistivity, ρ . For a tangential discontinuity, the theory predicts a depression in B, centered at the discontinuity, when $\omega \geq \omega_0 = \cos^{-1} \left[\frac{B_{\infty}^{-}}{2B_{\infty}^{+}} - \left(\frac{B_{\infty}^{-}}{B_{\infty}^{+}} \right)^{-1} \right]$, and it predicts a monotonic transition from B_{∞}^{-} to B_{∞}^{+} when $\omega < \omega_0$. The theory provides satisfactory fits to the magnetic field intensity and proton temperature profiles observed for two extremely broad D-sheets in the solar wind, using values of ρt (t being the "diffusion" time) determined by the observed widths of the profiles. Assuming that $t < 10$ days, one obtains effective resistivities $\rho \geq 3 \times 10^{12}$ emu and $\rho \geq 2 \times 10^{13}$ emu for these two D-sheets. Since most interplanetary "discontinuities" are at least an order of magnitude thinner than the D-sheet analyzed here, either the average resistivity at directional discontinuities is much lower than 10^{12} emu or annihilation does not always occur at discontinuities.

II

I. Introduction

Burlaga and Ness (1968) and Burlaga (1968) identified structures in the interplanetary magnetic field with dimensions $\leq .001$ AU which are characterized by a region of depressed magnetic field intensity, B , centered at a discontinuous change in the direction of the field (see Figure 1). They presented evidence that these structures, called D-sheets, result from annihilation of components of the magnetic field at the directional discontinuity, and they suggested that the broad depression in B is due to dissipation of field components near this discontinuity resulting from a non-zero electrical resistivity of the plasma. This paper develops these ideas further, with emphasis on the effects of dissipation.

Section II presents the theory for dissipation near a directional discontinuity and gives several theoretical profiles for $B(x,t)$. Section III applies this theory to published observations of two D-sheets and obtains a lower limit on the effective resistivity at these D-sheets. Section IV shows that these resistivities are much larger than those calculated from the Spitzer formula, but comparable to the anomalous resistivities given by Scarf, 1970.

The broad D-sheets discussed below are not frequently seen. Statistical studies have not been made, but it seems that they pass the earth at the rate of ≈ 1 /month, approximately the same rate as shock waves. Thus the resistivities derived from these D-sheets are not representative of the interplanetary plasma; however, we believe that D-sheets, like shock waves, are of considerable physical interest in themselves, and it is in this spirit that this paper is written.

II. Theory

The physical process which is formulated below is as follows. We assume that at a directional discontinuity in the solar wind, magnetic field is annihilated; the annihilation process determines the magnetic field intensity at the discontinuity. This intensity necessarily differs from the magnetic field intensity at $\pm\infty$, and consequently there are gradients of B near the discontinuity. We postulate that the electrical resistivity near the discontinuity is non-zero and finite, but constant. Under these conditions, magnetic field is dissipated, and the D-sheet broadens with a characteristic profile. We obtain a theoretical profile which can be compared with observations and can be used to determine the effective resistivity.

The geometry of the problem to be considered is illustrated in Figure 1. We consider a plane discontinuity surface corresponding to a directional discontinuity. Let the origin be on this surface, and let \hat{x} be the direction normal to the surface. Let the magnetic field intensity and temperature depend only on x and t, i.e., $B = B(x,t)$, $T = \pm T(x,t)$, where + refers to the region $x > 0$ and - refers to the region $x < 0$. $\pm T$ is the sum of the proton temperature, $\pm T_p$, and electron temperature, $\pm T_e$. Let $\underline{B} \rightarrow \pm \underline{B}_\infty$ as $x \rightarrow \pm \infty$, where $\pm \underline{B}_\infty$ are constant vectors along $\pm \hat{y}$, and let $+B > -B$, thereby defining \hat{x} .

We consider D-sheets for which the total pressure is constant,

$$\underline{P} = \pm nk (\pm T_e + \pm T_p) + \pm B^2 / (8\pi) = \text{constant} \quad (1)$$

This is the case for tangential and rotational discontinuities.

The momentum equation implies that the component of bulk velocity normal to the surface is constant. In a frame moving with the discontinuity surface, this is zero. The mass conservation equation then implies that $\partial n / \partial t = 0$, where n is the number density. Thus $n = n(x)$, independent of time. Changes in B as a function of time will be accompanied by changes in $T_p + T_e$, in accordance with (1), assuming negligible heat conduction; the magnetic energy which is dissipated appears as plasma thermal energy so that the total energy density does not change. Since the total pressure remains constant, there are no bulk motions.

Assume that at the directional discontinuity a component of the magnetic field is annihilated as discussed by Burlaga and Ness (1968). For a tangential discontinuity, $+\underline{B}_\infty$ and $-\underline{B}_\infty$ are parallel to the surface but not necessarily parallel to one another, and

$$|\underline{B}(0,t)| \equiv |\underline{B}_{\min}| = \left[+B_\infty^2 + -B_\infty^2 + 2\underline{-B}_\infty \cdot \underline{+B}_\infty \right]^{1/2} \quad (2)$$

$$\cos \omega \equiv \underline{-B}_\infty^\wedge \cdot \underline{+B}_\infty^\wedge$$

where ω is the angle between $+\underline{B}$ and $-\underline{B}$. For a rotational discontinuity, there is by definition a non-zero component of \underline{B} normal to the surface, \underline{B}_\perp , which is continuous across the surface [assuming thermal isotropy (Burlaga, 1971a)]. Only the components of \underline{B} parallel to the surface can be annihilated. Thus, for a rotational discontinuity,

$$B(0,t) = |\underline{B}_{\min}| = \left\{ B_{\perp}^2 + (\underline{B}_{\parallel\infty}^+)^2 + \underline{B}_{\parallel\infty}^-^2 + 2 \underline{B}_{\parallel\infty}^- \cdot \underline{B}_{\parallel\infty}^+ / 4 \right\}^{1/2} \quad (3)$$

$$\cos \omega = \frac{\underline{B}_{\parallel\infty}^-}{|\underline{B}_{\parallel\infty}^-|} \cdot \frac{\underline{B}_{\parallel\infty}^+}{|\underline{B}_{\parallel\infty}^+|}$$

Both (2) and (3) can be expressed as $\underline{B}_{\min} = (\underline{B}_{\infty}^- + \underline{B}_{\infty}^+)/2$; this relation does not involve the current sheet normal, which is not readily determinable for rotational discontinuities. The inner boundary condition is taken to be $\underline{B}^+(0,t) = B_{\min} \underline{B}_{\infty}^+ / |\underline{B}_{\infty}^+|$ for the solution $\underline{B}^+(x,t)$ in $x > 0$ and $\underline{B}^-(0,t) = B_{\min} \underline{B}_{\infty}^- / |\underline{B}_{\infty}^-|$ for the solution $\underline{B}^-(x,t)$ in $x < 0$. Thus, we assume no change in magnitude across the current sheet, but we postulate a non-zero change in direction (see Figure 1).

Assume that initially $\underline{B}^+(x)$ and $\underline{B}^-(x)$ are constant, equal to \underline{B}_{∞}^+ and \underline{B}_{∞}^- , respectively, and assume that the densities in the regions $x > 0$ and $x < 0$ are constant, equal to \underline{n}^+ and \underline{n}^- , respectively. The densities do not change with time, as discussed above.

The equation describing changes in the magnetic field is

$$\frac{\partial \underline{B}(x,t)}{\partial t} = \frac{\partial}{\partial x} \left(\eta \frac{\partial \underline{B}}{\partial x} (x,t) \right) \quad (4)$$

where

$$\eta = \rho / 4\pi \quad (5)$$

ρ being the electrical resistivity defined by $J_z = E_z/\rho$ in emu, Cowling (1957). This equation can be solved separately for the regions $x \geq 0$ and $x \leq 0$, and since B_{\perp} is either constant or zero, (4) may be regarded as an equation for the intensity of the magnetic field component parallel to the surface, $B_{\parallel}(x,t)$. For a tangential discontinuity, this is simply the total intensity of the magnetic field $|B_{\parallel}| = B(x,t)$. For a rotational discontinuity, the total magnetic field intensity is $B(x,t) = (B_{\perp}^2 + B_{\parallel}^2(x,t))^{1/2}$, where B_{\perp} is a constant not equal to zero, which is determined by the initial conditions.

Solving (4) for constant η subject to the above boundary conditions and initial conditions gives

$$B_{\parallel}^+ = B_{\parallel \min} + A \operatorname{erf}(\zeta) \quad x \geq 0 \quad (6)$$

and

$$B_{\parallel}^- = B_{\parallel \min} - A \operatorname{erf}(\zeta) \quad x \leq 0 \quad (7)$$

where

$$A = B_{\parallel} - B_{\min} \quad (8)$$

and

$$\zeta = x/(2\sqrt{\eta t}) \quad (9)$$

Figure 2a shows $B(\zeta, t)$ for the case ${}^+B_\infty = {}^-B_\infty$, $B_\perp = 0$, for several values of ω . Figure 2b shows the corresponding results for ${}^-B = {}^+B/2$, $B_\perp = 0$. As illustrated by Figure 2a, there need not be a depression in B at $x = 0$ if ${}^-B_\infty \neq {}^+B_\infty$. In fact, there will be no depression whenever $\omega < \omega_0 = \cos^{-1} (3R/2 - (2R)^{-1})$, where $R = {}^-B_\infty / {}^+B_\infty$. For example, if $R = .5$, $\omega_0 = 105^\circ$. When $\omega = 0$, there is simply a gradual, monotonic increase from ${}^-B_\infty$ to ${}^+B_\infty$, due to magnetic "diffusion". Figures 2a and 2b show the interesting facts that $B(\zeta)$ varies nearly linearly with ζ for small ζ and $\partial B / \partial \zeta \neq 0$ at $\zeta = 0$. This can be shown by using the series expansion for $\text{erf}(\zeta)$, which gives for small ζ

$${}^\pm B(\zeta) = B_{\min} + {}^\pm A (2\zeta / \sqrt{\pi} (1 + \zeta^2/3 + O(\zeta^4))) \quad (10)$$

In order to apply the above theory, it is necessary to determine whether the discontinuity under consideration is tangential or rotational. It is usually sufficient to determine whether or not the following necessary condition for rotational discontinuities is satisfied:

$${}^-V_\infty - {}^+V_\infty = \pm \left(\frac{{}^-B_\infty}{\rho_\infty} - \frac{{}^+B_\infty}{\rho_\infty} \right) \left(\frac{{}^-B_\infty}{4\pi} \right)^{1/2} \left\{ 1 - \frac{({}^-P_{\parallel\infty} - {}^-P_{\perp\infty}) 4\pi}{{}^-B_\infty^2} \right\}^{1/2} \quad (11)$$

where ${}^-P_{\parallel\infty}$ and ${}^-P_{\perp\infty}$ are the total thermal pressures parallel and perpendicular to ${}^-B$, (Hudson, 1970). If this condition is not satisfied, the discontinuity is tangential (assuming that discontinuities with shock-signatures have been excluded). Other bounds for rotational discontinuities under conditions at 1 AU are given by Hudson (1972).

III. Observations

To relate the above theory to observations, one must consider that the discontinuity surface moves past the observer and that \hat{x} can be in any direction. For a tangential discontinuity, the spatial scale of an observed profile is $|\underline{x}| = |\underline{v} \cdot \hat{x}| \tau$, where \underline{v} is the solar wind velocity, $\tau \equiv |t - t_0|$ is the time relative to the time t_0 of the passage of the discontinuity, and $\hat{x} = -(\underline{B}^+ \times \underline{B}^-) / |\underline{B}^+ \times \underline{B}^-|$.

Collecting the above results gives for a tangential discontinuity:

$$\pm B(\tau) = B_{\min} + (\pm B_{\infty} - B_{\min}) \operatorname{erf}(\pm \alpha \tau) \quad (12)$$

where

$$\pm \alpha = \pm \underline{v} \cdot \hat{x} / (2 \sqrt{\eta t}) \quad (13)$$

It is assumed that $t \gg \tau$, i.e., that the elapsed time t since the formation of the current sheet, is larger than the time interval τ during which the D-sheet moves past the spacecraft. If D-sheets, like directional discontinuities, are formed within .8 AU (Burlaga, 1971b), then this condition is met by orders of magnitude. When $(\pm \alpha \tau)^2 \ll 3$ one can use the series expansion for the error function (see Eq. 10) to relate $\pm \alpha$ to the "half-width" $\pm \tau_w$ the $\pm \tau$ at which $\pm B = B_{\min} + (\pm B - B_{\min})/2$.

The result is

$$\pm \alpha = \frac{\sqrt{\pi}}{4(\pm \tau)} = .443 / (\pm \tau_w) \quad (14)$$

Comparing (13) and (14) gives the important result that if η is constant ($+\eta = -\eta$), and if $t \ll \tau$, then $+\tau_w = -\tau_w \equiv \tau_w$.

Thus, $\vec{B}(t)$ and ${}^+B(t)$ are determined by four measurable constants: τ_w , B_{\min} , and ${}^+B$. In particular, if ${}^+B(\tau)$ is calculated from τ_w , B_{\min} , and ${}^+B_{\infty}$, then $\vec{B}(\tau)$ is determined by only one additional number, \vec{B}_{∞} . Given ${}^+B(t)$, the temperature can be calculated from (11) and compared with observations.

April 3, 1966, Event. Figure 2 shows a D-sheet which was convected past Pioneer 6 on April 3, 1966. The data differ only slightly from the preliminary results in Burlaga (1968). As indicated by the bottom panel of Figure 2, the total pressure computed assuming a constant electron temperature, $T_e = 1.7 \times 10^5$ °K, (Montgomery 1972; Scudder et al., 1972), is constant within the experimental uncertainties, as required by the theory in Section II. From Figure 2 we take B , θ and φ equal to 4.4γ , -35° , 180° , respectively for \vec{B}_{∞} and 6.8γ , 20° , 350° , respectively for ${}^+B_{\infty}$. In solar ecliptic (GSE) coordinates (\hat{x} toward the sun, \hat{z} normal to the ecliptic and \hat{y} to form a right-handed system), $\vec{B} = (3.6, 0.0, 2.5)$ and ${}^+B = (6.3, -1.1, +2.3)$. The angle between \vec{B} and ${}^+B$ is $\omega = 175^\circ \pm 15^\circ$.

To determine whether or not the discontinuity is rotational, consider (11). If the pressure were isotropic, the change in the radial component of the solar wind velocity should be $|\vec{v}^- - \vec{v}^+| = 115$ km/sec if the discontinuity were rotational. In fact, the solar wind pressure is anisotropic, but the anisotropy was not measured for the event under consideration. Typically, however, $4\pi (P_{\parallel} - P_{\perp})/B^2 \approx .1$ (e.g., see Hundhausen, 1972). Thus, if the discontinuity were rotational, one expects $|\vec{v}_{\infty}^- - \vec{v}_{\infty}^+| \approx 105$ km/sec. This is much larger than the observed

value, $|\Delta V| \approx 10$ km/sec, so we conclude that the discontinuity is tangential.

The theoretical value of B_{\min} , given by (2), is $\approx 1.2\gamma$ for $\omega = 175^\circ$, $\bar{B}_\infty = 4.4\gamma$, ${}^+B_\infty = 6.8\gamma$. The uncertainty in ω is approximately 15° , and the corresponding uncertainty in B_{\min} is $\approx \pm 0.3\gamma$. Thus, the theoretical B_{\min} , computed from the annihilation hypotheses, is consistent with the observed $B_{\min} = 0.9\gamma$.

${}^+B(\tau)$ was computed from (12) using the observed B_{\min} and ${}^+B_\infty$ and taking the "half-width" of ${}^+B_\infty$ to be $\tau_w = 1.3$ min. The result, shown in Figure 3, is in excellent agreement with the observations. Using only one additional quantity $\bar{B}_\infty = 4.4\gamma$, $\bar{B}(\tau)$ was computed from (12), with the result shown in Figure 3. Again, the result is in excellent agreement with observations. Note that no free parameters were used to obtain this result.

The theoretical proton temperature profile (computed from the observed densities, the theoretical $B(\tau)$, and the assumption that $T_e = \text{constant} = 1.7 \times 10^5$ °K) is shown in Figure 3. There is qualitative agreement with observations in that the theory predicts a maximum in proton temperature at the directional discontinuity, consistent with a large increase in temperature which is observed there. However, this conclusion is based on only one measurement, and the uncertainties in this measurement are very large. Furthermore, in the absence of electron measurements we cannot exclude the possibility that electrons are also heated at the current sheet. With such data, one cannot be certain that heat conduction is insignificant.

December 27, 1965, event. Figure 4 shows a D-sheet which was convected past Pioneer 6 on December 27, 1965. This was mentioned in the papers by Burlaga and Ness (1968) and Burlaga (1968), but the data here are more complete and are presented in an extended format of Figure 3. The total pressure (plasma plus field) is essentially constant if we assume $T_{e\infty}^- = 1.50 \times 10^5$ °K, $T_{e\infty}^+ = 1.86 \times 10^5$ °K, which are both within the range of reported solar wind electron temperatures, (Montgomery 1972, Scudder et al., 1972). For \underline{B}_∞^- and \underline{B}_∞^+ we take, (B, θ_{se} , ϕ_{sw}) = (5.85 γ , +10°, 100°) and (6.0 γ , -20°, 185°), respectively. In GSE rectangular coordinates these yield $\underline{B}^- = (-1.0, 5.67, 1.0)\gamma$ and $\underline{B}^+ = (-5.61, -0.49, -2.0)\gamma$. For \underline{V}^- and \underline{V}^+ we have taken (-587, -10, -45) km/sec and (-563, 20, -25) km/sec, respectively. To determine the nature of this discontinuity we use Eq. (11) neglecting the pressure anisotropy to compute the $\Delta\underline{V}_r$ necessary for the discontinuity to be rotational: $\Delta\underline{V}_r = (51, 74, 35)$ km/sec. $\Delta\underline{V}_{\text{observed}} = (-24 \pm 5, -30 \pm 20, -20 \pm 20)$ km/sec. A pressure anisotropy of 1.4×10^{-10} ergs/cm³ is required to force equality. This is clearly unreasonable since it exceeds the total plasma pressure for a $\beta = 1$ plasma with $B = 5.8\gamma$, which is 1.35×10^{-10} ergs/cm³. Even a mixture of more reasonable anisotropic effects plus experimental errors could not make the equivalence. We therefore tentatively conclude that this is a tangential discontinuity. The different electron temperatures adopted are also reasonably interpreted as being characteristic of two distinct regions of plasma with a non-propagating (tangential discontinuity) interface. As a check on this conclusion we test a necessary condition for a tangential discontinuity:

$\Delta V_{\infty} \cdot (\underline{B}_{\infty}^{-} \times \underline{B}_{\infty}^{+}) = 0$. For the values chosen $\frac{\Delta V_{\infty} \cdot (\underline{B}_{\infty}^{-} \times \underline{B}_{\infty}^{+})}{|\Delta V_{\infty}| |\underline{B}_{\infty}^{-} \times \underline{B}_{\infty}^{+}|} = -.09 \begin{pmatrix} +.47 \\ -.12 \end{pmatrix}$

which is consistent with our initial conclusion that the discontinuity is tangential.

The components of \underline{B}_{\min} as interpolated across the discontinuity (Figure 4) give no new information about the classification, since by the generalization of Equations (2) and (3) the components of \underline{B}_{\min} are determined in the same way from \underline{B} for the two classes. The components of the vector \underline{B}_{\min} are indicated by the dashed lines in the \underline{B} field rectangular components panels of Figure 4. Since each point there represents $\langle B_i \rangle_t$ over 15 secs, the agreement with theory is good. The total field plotted is $\langle (\sum B_i^2)^{1/2} \rangle_t$. Thus a reasonable empirical $\underline{B}_{\min} (\tau = 0)$ is $(-2.0 + 3.5, +0.5)$, yielding $|\underline{B}_{\min}| = 4.1 \pm 0.2\gamma$. Using this value of \underline{B}_{\min} yields a reasonable theoretical agreement for the remainder of the empirical data.

We thus proceed on the supposition that the discontinuity is tangential with $^+A = 1.8\gamma$, $^-A = 1.65\gamma$, $^{\pm}\tau_w = \tau_w = .5$ min, and $\alpha = .886$, which yields the theoretical field profiles in the left hand panels of Figure 4. The theory qualitatively reproduces most temperature variations near and far from the sheet.

The main discrepancies from theoretical profiles occur in the wings of the profile. A spatially dependent resistivity is probably required to explain the entire profile in detail. The basic features of this theory, suitably extended to accommodate $\rho(\zeta$ and/or number density) seems capable of explaining some of the observed D-sheet structures in the solar wind.

B

IV. Discussion

It was shown above that for two D-sheets in the solar wind near 1 AU, the observed $B(t)$ profiles are quantitatively in agreement with a theory which postulates magnetic field annihilation at a directional discontinuity and resistive dissipation of magnetic field gradients near the discontinuity. The theory predicts a depression in B at the current sheet when $\omega > \cos^{-1} (3R/2 - (2R)^{-1})$, where $R \equiv \bar{B}_\infty / {}^+B_\infty < 1$. Furthermore, it predicts that the "half-widths" of $\bar{B}(t)$ and ${}^+B(t)$ should be equal for constant $|\underline{V} \cdot \hat{x}|$ and η , (${}^+\tau_w = \tau_w \equiv \tau_w$), and that τ_w is related to the electrical resistivity by (5), (13) and (14) i.e.,

$$\rho = 16 (\underline{V} \cdot \hat{x})^2 \tau_w^2 / t \quad (15)$$

The value of t , the length of time during which magnetic diffusion has been occurring, is unknown, but is probably less than the time required for an element of the solar wind to move from the sun to 1 AU which is presumably less than 10 days. If this is correct, the theory gives a lower limit on ρ

$$\rho > 16 (\underline{V} \cdot \hat{x})^2 \tau_w^2 / t_{10} = (\underline{V} \cdot \hat{x})^2 \tau_w^2 \times 6.6 \times 10^8 \quad (16)$$

where V is in km/sec and τ_w is in min in the last equality.

For the April 3, 1966, event: $V = 415 \pm 5$ km/sec, $|\underline{V} \cdot \hat{x}| \approx 128$ km/sec which gives

$$\rho \geq 2 \times 10^{13} \text{ emu} \quad (17)$$

For the December 27, 1965, event, $V = 575 \pm 15 \text{ km/sec}$, $\hat{x} = (0.32, 0.22, -.92)$, and $\tau_w = 0.5 \text{ min}$, giving

$$\rho \geq 3 \times 10^{12} \text{ emu} \quad (18)$$

The values of ρ given above represent limits on the effective resistivity derived from a macroscopic model with a very specific geometry. Currents do not appear explicitly in the basic equations, but it can be shown that the constraint $\underline{B} = B(x)\hat{y}$ implies that the induced electrical field, \underline{E} , (\underline{E} is not impressed externally) will not necessarily be along the current \underline{J} , so the elementary concept of resistivity does not apply here. The situation is further complicated in that $\omega_e t_e \gg 1$, where ω_e is the electron gyrofrequency and t_e is the electron-proton collision time; Chapman and Cowling (1970) point out that "It is, questionable whether the concept of conductivity has any real significance when $\omega_e t_e$ is large". Finally, it is believed that in a collisionless plasma such as the solar wind the classical Spitzer-Härm formula for a fully ionized plasma is probably not applicable because of the growth of various microinstabilities (Schindler, 1972; Scarf, 1970). Comparing our empirical resistivities with those given by the Spitzer-Härm formula (Spitzer, 1962) we find that for $T = 2 \times 10^5 \text{ }^\circ\text{K}$, $\rho \approx 2 \times 10^6 \text{ emu}$,

and for $T \approx 6 \times 10^4$ °K, $\rho \approx 10^7$ emu.; these values of ρ are on the order of six orders of magnitude smaller than the lower limits obtained from the observations. On the other hand, using the effective collision frequency for ion sound waves with strong turbulence (Scarf, 1970) we find 2×10^{14} emu, which is 1 to 2 orders of magnitude larger than, but still consistent with, our empirical lower bounds.

We emphasize that the values of ρ given by (17) and (18) are not representative of the solar wind plasma near 1 AU. If they were representative, all directional discontinuities would show the effects described in Section II, contrary to observations. If annihilation and diffusion do occur at most directional discontinuities in the solar wind, τ_w is typically $\ll 2$ min. In fact, inspection of high resolution IMP I data shows that typically $\tau_w < 1$ sec. The normal effective resistivity is correspondingly much smaller than the value 10^{12} to 10^{13} emu derived above and could, in fact, be consistent with the Spitzer (1962)-Braginskii (1968) result.

Finally, we note that the theory presented and applied in this paper may not be valid for all D-sheets. It was assumed that pressure is absolutely constant and that heat conduction is negligible, which implies no bulk motion and no change in density. However, observations of some D-sheets (Burlaga, 1970) show an appreciable enhancement in density, but no comparable increase in temperature at the corresponding discontinuities. This would occur if heat were conducted away and material were conducted away and material were convected toward the discontinuity. The theory of this more complex process will be presented in a subsequent paper.

Acknowledgements

The plasma and magnetic field are from the experiments of Bridge (MIT) and Ness (GSFC), respectively. Dr. Lazarus provided and discussed the plasma data. Valuable comments on the manuscript were contributed by Ogilvie and Ness.

References

- Braginskii, S. I., Transport Processes in a Plasma, Rev. Plasma Physics, 1, 205, 1968.
- Burlaga, L. F., Microscale Structures in the Interplanetary Medium, Solar Phys. 4, 67, 1968.
- Burlaga, L. F., Hydromagnetic Waves and Discontinuities in the Solar Wind, Space Science Rev., 12, 600, 1971a.
- Burlaga, L. F., On the Nature and Origin of Directional Discontinuities, J. Geophys. Res., 76, 7516, 1971b.
- Burlaga, L. F. and K. W. Ogilvie, Magnetic and Thermal Pressures in the Solar Wind, Solar Physics, 15, 61, 1970 .
- Burlaga, L. F. and N. F. Ness, Macro and Micro-Structure of the Interplanetary Magnetic Field, Can. J. Phys. 46, 5962, 1968.
- Chapman, S. and Cowling, The Mathematical Theory of Non-Uniform Gasses, Cambridge University Press, 1970.
- Cowling, T. G., Magnetohydrodynamics, Interscience, 1957.
- Hudson, P. D., Discontinuities in an Anisotropic Plasma and Their Identification in the Solar Wind, Planet. Space Sci., 18, 1611, 1970.
- Hudson, P. D., Rotational Discontinuities in an Anisotropic Plasma II, in press, Planet. Space Sci., 1972.
- Hundhausen, A. J., Coronal Expansion and the Solar Wind, Springer-Verlag, 1972.
- Montgomery, M. D., Average Thermal Characteristics of Solar Wind Electrons, in Solar Wind, Sonett, Coleman, and Wilcox eds., NASA SP-308, 208, 1972.

Scarf, F. L. Microscopic Structure of the Solar Wind, Space Science.

Rev., 11, 234, 1970.

Schindler, K., Magnetic Field Merging in the Solar Wind, in The Solar Wind,

Sonett, Coleman and Wilcox, eds. NASA SP-308, 360, 1972.

Scudder, J. D., D. Lind, and K. W. Ogilvie, Electron Observations in the

Solar Wind and Magnetosheath, submitted to J. Geophys. Res., 1972.

Spitzer, L., Physics of Fully Ionized Gases, Interscience, New York, 1962.

Figure Captions

Figure 1 Shown is the geometry of the current annihilation model for either a rotational (RD) or tangential (TD) discontinuity. If it represents a TD, $\underline{B}_{\parallel}(x) = \underline{B}(x)$; if a (RD) $\underline{B}_{\parallel}(x) = \underline{B}(x) - \underline{B}_{\perp}$. The magnitude of $\underline{B}(0)$ results from the annihilation of components of $\underline{B}_{\parallel}$ after the suggestion of Burlaga and Ness (1968). In general $\underline{B}(0) = \underline{B}_{\parallel}(0) + \underline{B}_{\perp} = 1/2 (\underline{B}_{\parallel\infty}^+ + \underline{B}_{\parallel\infty}^-)$; this implies $\underline{B}_{\parallel}(0) = 1/2 (\underline{B}_{\parallel\infty}^+ + \underline{B}_{\parallel\infty}^-)$ as is shown.

Figure 2 Shown are theoretical profiles for annihilation models with no fluid motion relative to the surface and varying angles $\omega = \cos^{-1}(\underline{B}_{\parallel\infty}^+ \cdot \underline{B}_{\parallel\infty}^-)$ for $|\underline{B}_{\parallel}^+|, |\underline{B}_{\parallel}^-| = 1, 2$ on left and right hand sides respectively. ζ is the dimensionless space-time variable defined in the text by Eq. 9. The profiles for rotational discontinuities may be determined via defining $B_{\perp}/B_{\parallel\infty}$ and then $|\underline{B}(x)| = (B_{\parallel}^2(x) + B_{\perp}^2)^{1/2}$, giving a less steep profile.

Figure 3 April 3, 1966, Event: Empirical field and particle profiles (dots) from Pioneer VI compared with theory (solid curves).

Figure 4 December 27, 1965, Event: Full data set used in determining type of discontinuity. Resultant comparison between relevant form of theory and empirical data are shown by solid curves.

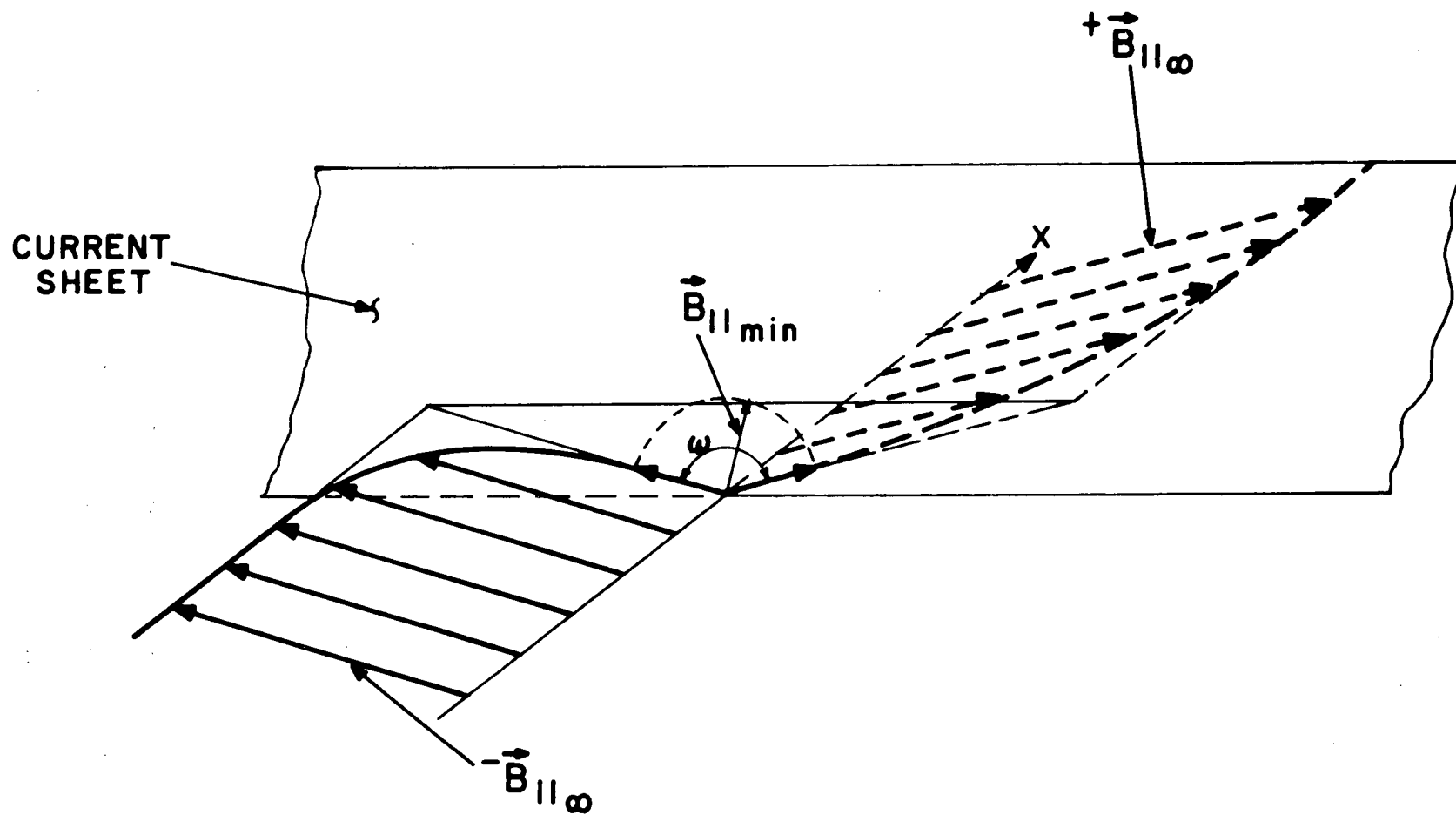


FIGURE 1

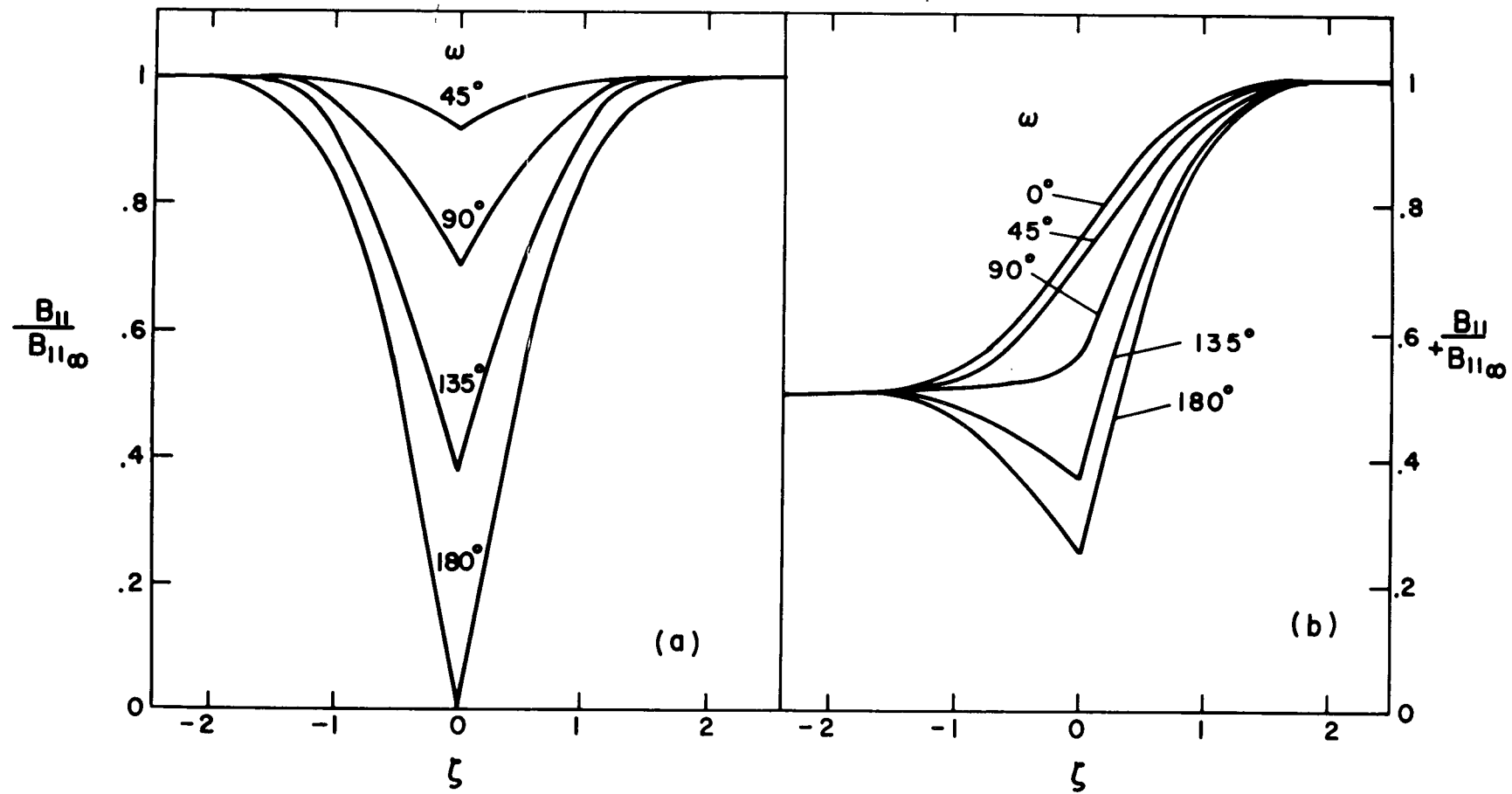


FIGURE 2

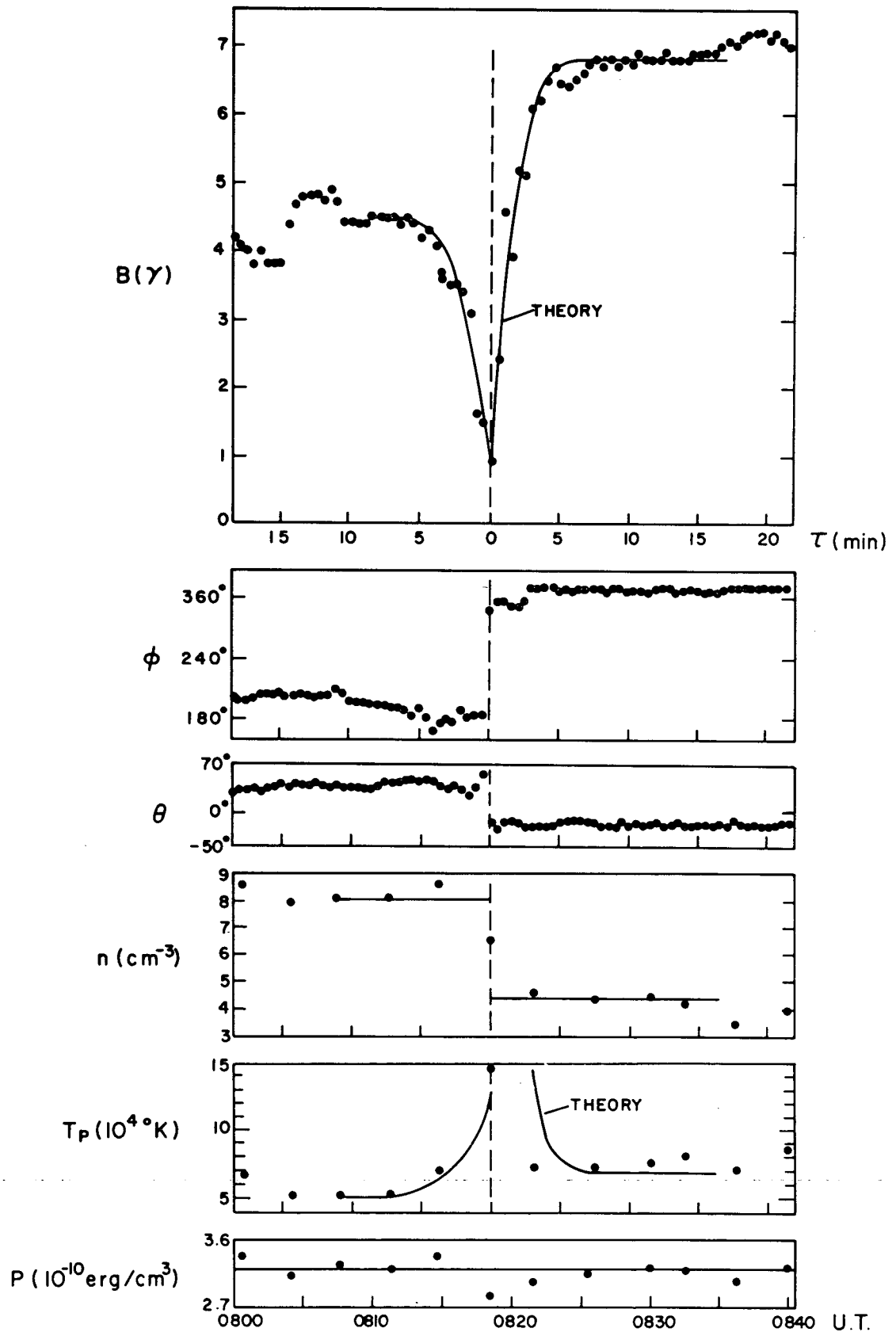


FIGURE 3

DEC. 27, 1965

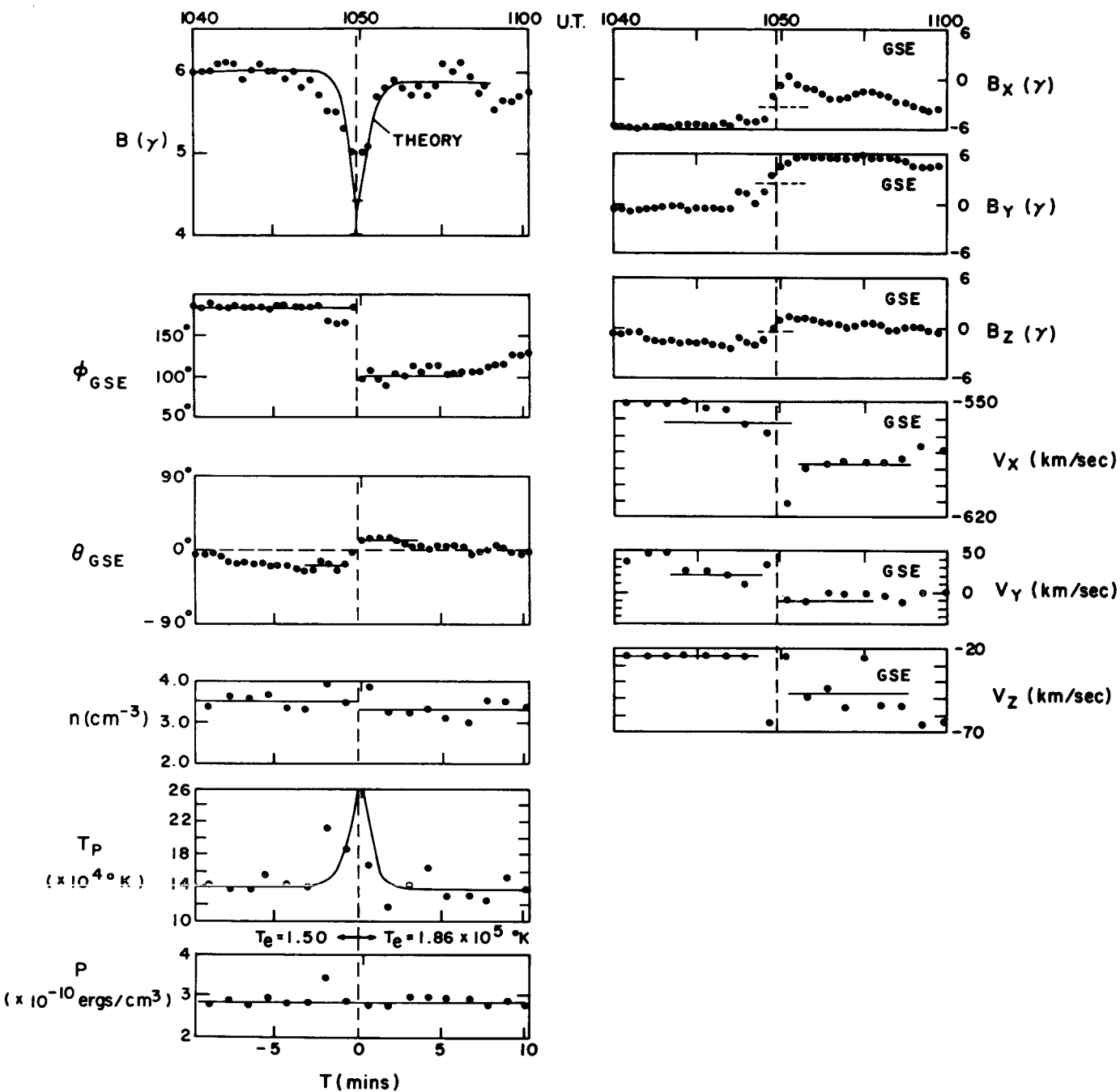


FIGURE 4

NASA-GSFC